Cite this: *Lab Chip*, 2011, **11**, 2432

www.rsc.org/loc

PAPER

Microfluidic array cytometer based on refractive optical tweezers for parallel trapping, imaging and sorting of individual cells†

Michael Werner,[a] Fabrice Merenda,‡[b] Joachim Piguet,[a] René-Paul Salathé[b] and Horst Vogel*[a]

Received 2nd March 2011, Accepted 6th May 2011
DOI: 10.1039/c1lc20181f

Analysis of genetic and functional variability in populations of living cells requires experimental techniques capable of monitoring cellular processes such as cell signaling of many single cells in parallel while offering the possibility to sort interesting cell phenotypes for further investigations. Although flow cytometry is able to sequentially probe and sort thousands of cells per second, dynamic processes cannot be experimentally accessed on single cells due to the sub-second sampling time. Cellular dynamics can be measured by image cytometry of surface-immobilized cells, however, cell sorting is complicated under these conditions due to cell attachment. We here developed a cytometric tool based on refractive multiple optical tweezers combined with microfluidics and optical microscopy. We demonstrate contact-free immobilization of more than 200 yeast cells into a high-density array of optical traps in a microfluidic chip. The cell array could be moved to specific locations of the chip enabling us to expose in a controlled manner the cells to reagents and to analyze the responses of individual cells in a highly parallel format using fluorescence microscopy. We further established a method to sort single cells within the microfluidic device using an additional steerable optical trap. Ratiometric fluorescence imaging of intracellular pH of trapped yeast cells allowed us on the one hand to measure the effect of the trapping laser on the cells' viability and on the other hand to probe the dynamic response of the cells upon glucose sensing.

1 Introduction

The physiological properties of cells are typically investigated in ensembles yielding averaged data that mask heterogeneities present in any cell population.[1–3] Although still at a very early stage, single-cell analyses have provided intriguing results which could not be obtained from averaged population properties revealing biological importance of cell variability. For instance, within a cell population expression levels of genes, concentrations of intracellular components or intracellular response patterns upon extracellular stimuli can vary strongly from cell to cell.[4–8] Cellular heterogeneity can be caused by genetic variability, asynchronous cell-cycle and different microenvironments, or simply by the stochastic nature of molecular processes.[6,9–11] Investigating cellular variability, elucidating the molecular principles governing a cell's functional or, in the case of disease, dysfunctional characteristics are central objectives of systems biology.[12] This, however, requires experimental techniques allowing to efficiently monitor cell-to-cell variability of the response of a cell population to external stimuli and to sort out interesting cell phenotypes for further investigation, *e.g.* gene expression analysis. Fluorescence-activated-cell-sorting (FACS) is a widely used technique enabling combined screening and sorting of single cells at rates as high as 50.000 s^{-1}.[13,14] Even though FACS is a mature technique advanced during 40 years of continuous development, its inherent limitations like requirement of large sample size (> 10^5 cells) and high costs have led in recent years to the development of microfluidic cell sorters (μFACS).[15–17] However, a bottleneck of classical and miniaturized flow-cytometric sorters is their restriction to single-point measurements lacking ability to resolve the dynamic responses of single cells over time.[18] To follow dynamic processes in single cells, they have to be kept in a fixed position for minutes, hours or even days. Fluorescence-based image cytometry[19] of cells randomely distributed on microscope slides or densely packed in microfabricated array cytometers[20–22] provide such measurements. Several strategies were also developed to isolate single cells of interest using micromanipulators[22–24] or laser-capture microdissection.[25,26] However, apart from the fact that cell attachment is often irreversible, those methods are slow and difficult to apply to non-adherent cells.[27] For these reasons, new methods for cell patterning and cell manipulation have recently

[a]*Laboratory of Physical Chemistry of Polymers and Membranes, Ecole Polytechnique Fédérale de Lausanne (EPFL), Lausanne, Switzerland. E-mail: horst.vogel@epfl.ch*
[b]*Advanced Photonics Laboratory, Ecole Polytechnique Fédérale de Lausanne (EPFL), Lausanne, Switzerland*

† Electronic supplementary information (ESI) available: Movie1.mov: multiple optical trapping of yeast cells in microfluidics (2× accelerated). Movie2.mov: lateral displacement of the cell array in the microfluidic device (2× accelerated). See DOI: 10.1039/c1lc20181f

‡ Present address: Arcoptix S.A., Neuchâtel, Switzerland.

been introduced using hydrodynamic trapping,[28] or magnetic,[29] acoustic,[30] dielectrophoretic[18,31–33] and optical tweezers.[34] These methods are suited for adherent as well as non-adherent cells, and can be combined with other techniques like fluorescence microscopy or spectroscopy. Moreover, their integration into microfluidic systems provides fast and controlled transport of specimen and reagents yielding highly versatile array cytometers.

A disadvantage of hydrodynamic trapping, though, is that cells can irreversibly attach to the trapping sites rendering cell sorting difficult.[27] Magnetic and acoustic trapping can successfully pattern cells into large arrays, yet they still lack the ability to precisely manipulate single cells. Several instruments based on dielectrophoretic trapping proved to be able to monitor single-cell dynamics in parallel and to sort cells of interest, however, drawbacks are low cell survival rates[35] and expensive instrumentation. Starting from the seminal work of Ashkin *et al.*,[36] optical tweezers have shown their potential for trapping living cells to form regular arrays and for precise manipulation of single cells.[34,37–41] Multiple optical trap arrays are usually created by time-sharing of a single laser beam[42] or by using computer-generated diffraction patterns ("holographic tweezers").[43] Both methods generate multiple, individually addressable traps, but limited trap number and complex as well as expensive instrumentation still prevent optical tweezers from being used as a standard cytometric tool.

Addressing these shortcomings we here report on the development of a microfluidic array cytometer based on refractive multiple optical tweezers generated by inexpensive microlenses.[44–46] We demonstrate the ability of such optical trap arrays to immobilize more than 200 yeast cells in parallel. Single cells immobilized in the array could be individually manipulated and isolated. The experimental platform was easily combined with fluorescence microscopy enabling us to demonstrate its applicability for single-cell analysis by monitoring the dynamic response of the intracellular pH of yeast cells following glucose exposure.

2 Experimental

2.1 Experimental setup

2.1.1 Multiple optical tweezers and fluorescence microscopy. A scheme of the optical setup is depicted in Fig. 1A. An Ytterbium fiber laser with linear polarization (PYL-10-1064-LP, IPG Photonics) emitting up to 10 W cw at 1064 nm in a TEM_{00} mode was used for optical trapping. Multiple optical traps were generated by means of an array of fused silica microlenses (ML) manufactured by Süss MicroOptics (Neuchâtel, Switzerland). The microlenses (numerical aperture NA = 0.07) were arranged in a hexagonal array with a pitch of p = 250 μm. Laser light focused by each microlens in the array created a multitude of beamlets, which were subsequently re-collimated by a field lens (FL). The whole bundle of collimated beamlets spatially overlapped at the focal plane of the field lens, where the back aperture of the microscope objective (MO, C-Apochromat 40 × 1.2 W Corr UV-Vis-IR, Zeiss, Germany) should have been positioned. Due to the technical challenges to implement custom optics into a standard inverted microscope (Axiovert 200M, Zeiss, Germany), the bundle of beamlets was formed outside the microscope and then transfered to the microscope objective by a 4-f relay lens system

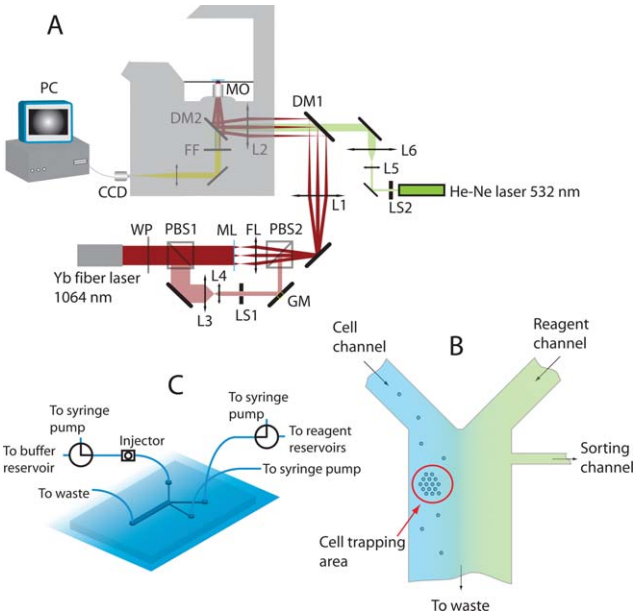

Fig. 1 Schematic description of (A) the optical setup, (B) the microfluidic chip, and (C) the fluidic circuit.

(L1, L2). This offered the additional advantage that laser light for fluorescence excitation could enter the microscope through the same port. As each beamlet entered the microscope objective at a different angle, the formed optical traps were spatially separated in a regular pattern according to the hexagonal microlens array. The spacing of the traps in the objective focal plane was ~ 10 μm.

An additional steerable optical trap was implemented. A polarizing beamsplitter (PBS1) split the principal light beam into two components with perpendicular polarizations. A rotatable λ/2-plate (WP) in front of the polarizing beamsplitter allowed to adjust the power taken from the initial laser to form the second beam. The latter beam passed a telescope (L3, L4) and merged with the optical pathway of the microlens-generated beam bundle through a second polarizing beamsplitter (PBS2). Lateral displacement of the single optical trap in the sample was controlled through a homebuilt galvanic mirror (GM), whose tilt could be controlled in two dimensions in front of the second polarizing beamsplitter. This mirror was positioned in an optical plane conjugated to the microscope objective back aperture ensuring that the quality of the trap would not degrade upon displacement in the sample. By making the beam slightly divergent at the back aperture of the microscope objective, the steerable optical trap was focused a few microns above the focal plane of the fixed trap array. This ensured that once a particle was captured by the steerable optical trap it could be manipulated freely without perturbation by the trap array. A laser shutter (LS1) allowed to switch on/off the steerable optical trap, independent from the optical trap array.

A He–Ne laser emitting at 532 nm (TECGL-30-532, GMP, Switzerland) was available for fluorescence excitation. After passing a laser shutter (LS2) the laser beam was expanded (L5, L6), coupled into the optical path of the IR laser by means of a dichroic mirror (DM1, Chroma, USA) and focused on the back focal plane of the objective thus illuminating an area of the sample corresponding to the objective's field of view. Infrared

trapping and fluorescence excitation laser light was separated from the emitted fluorescence light using a dielectric mirror (DM2, Chroma, USA) and appropriate fluorescence filters (FF). A CCD camera (Pixelfly, PCO, Germany or Andor Luca S, Andor Technology, N. Ireland) was used for fluorescence and brightfield imaging.

2.1.2 Microfluidic chip and system. The microfluidic chip was fabricated using soft lithography methods.[47] PDMS (Sylgard 184, Suter Swiss Composite Group, Switzerland) was cast on a master mold (Stanford Microfluidics Foundry, USA) and cured at 80 °C for 12 h. The PDMS slab was peeled off the master mold and holes (~1 mm in diameter) were punched at the inlets and outlets of the channels. The device was then sealed to a thin microscope cover-glass (150 μm thick). To achieve a tight seal, the contact surfaces of the PDMS and the cover-glass were rendered hydrophilic prior to bonding using oxygen plasma. The microfluidic chip used in all experiments (Fig. 1B) had two inlet channels (100 μm wide) merging into the main channel being 500 μm wide. A smaller channel (100 μm wide) diverged from the main channel. All channels were 50 μm high. The chip was clamped on a joystick-controlled motorized scanning stage.

Apart from the chip the microfluidic setup (Fig. 1C) consisted of syringes (Gastight 1705, Hamilton, USA), syringe pumps (SP 210iw, WPI, USA), tubings (FEP tubing 1526, Upchurch Scientific, USA) and valves (Omnifit 1120, Bio-Chem Fluidics, USA). The tubings were connected to the microfluidic chip by directly plugging one end of the tubings into the inlet and outlet holes of the device. Connections between tubings and valves were done *via* appropriate adapters (flangeless nuts/ferrules, Upchurch Scientific, USA). The chip was fed by two fluidic circuits. One fluidic circuit addressed the channel where particles were injected in the microfluidic chip; in the following it is referred to as the cell channel. It consisted of one pump driving a syringe connected to a 4-port valve that switched between the fluidic circuit or a cell buffer containing reservoir. An injector was interconnected in proximity to the chip inlet for injection of defined volumes (0.1–10 μL) of suspended cells. The second fluidic circuit, referred to as the reagent channel, addressed the channel where particles were exposed to reagents. Here the pump drove a syringe connected to a 4-port valve that switched between the fluidic circuit and reagents containing reservoirs. Flows from the cell channel and the reagent channel were merged in the main channel to yield two adjacent laminar flows. The third fluidic circuit, referred to as the sorting channel consisted of a syringe pump directly connected to the sorting channel of the microfluidic chip. The outlet of the main channel was connected to an open waste reservoir.

2.1.3 User interface. For controlling laser shutters, syringe pumps and the galvanic mirror a graphical user interface (GUI) was developed using commercially available software (LabView 8.5, National Instruments, USA) and hardware (USB-6009, National Instruments, USA). Using the GUI, feed rates of the syringe pumps could be precisely controlled and modified on-line. The position of the steerable beam in the field of view, given by the tilt of the galvanometric mirror, could be controlled by mouse clicks on the computer screen. The Pixelfly CCD camera was controlled by the homewritten GUI, whereas the Andor Luca S CCD camera was controlled by commercially available software (SOLIS 4.7, Andor Technology, N. Ireland).

2.2 Chemicals and buffers

SNARF-4F 5-(and-6)-carboxylic acid, acetoxymethyl ester, acetate was purchased from Molecular Probes, Amphotericin B from Sigma-Aldrich. McIllvaine buffers of different pH values were prepared by mixing appropriate volumes of 200 mM Na_2HPO_4 and 100 mM citric acid. A loading buffer was prepared by diluting an aliquot of a SNARF-4F stock solution (9.7 mM in DMSO) in McIllvaine buffer (pH 4) to a final concentration of 20 μM.

2.3 Cell culture

Yeast *S.cerevisiae* were grown on agar plates containing YPD medium (Clontech, USA). A cell colony was picked, inoculated in liquid YPD and grown overnight at 30 °C. After 24 h a 1 mL aliquot of the cell suspension was taken, centrifuged at 5000 rpm for 5 min and the cell pellet was resuspended in buffer.

2.4 Measurement of intracellular pH dynamics of optically trapped yeast cells

2.4.1 Fluorescence image acquisition and analysis. The optical probes were excited at 532 nm with ~3 mW. For each measurement two images with an exposure time of 200 ms were acquired using fluorescence emission filters transmitting fluorescence light in the range of 560–580 nm or 650–690 nm, respectively. A custom-built slide integrated in the microscope allowed to quickly switch between the fluorescence emission filters so that both images were taken with a delay of 2 s. For analysis images were background-substracted and ratiometric analysis was performed using homewritten software and ImageJ 1.43.

2.4.2 SNARF-4F loading of yeast cells. Yeast cells were loaded with SNARF-4F according to the protocol developed by Valli *et al.*[48] Yeast cells were suspended in 250 μL of loading buffer and incubated at 30 °C for 15 min in a shaker. The cells were collected by centrifugation at 5000 rpm for 5 min, resuspended in McIllvaine buffer (pH 4) if not stated otherwise, and then immediately analyzed.

2.4.3 *In situ* calibration of intracellular pH and measurement of intracellular pH against extracellular pH. Yeast cells loaded with SNARF-4F were split into 6 equal volumes and each aliquot was washed by centrifugation. The cell pellets were then resuspended in the same volume (250 μL) of fresh McIllvaine buffer adjusted to distinct pH values (4, 5, 6, 7, 8 and 9, respectively). For *in situ* calibration each cell suspension was additionally mixed with 1.5 μL of an Amphotericin B stock solution (5 mM in water), incubated for 1 h at 37 °C while shaking and then analyzed. For measuring the intracellular pH against the extracellular pH the samples were immediately analyzed.

A sample was analyzed by pipetting a drop of its content on a microscope cover slide. After sedimentation of the cells fluorescence images comprising 5 different regions of interest (ROI)

were taken. The fluorescence ratio of each ROI was determined and an average fluorescence ratio was calculated for the sample.

For *in situ* calibration average fluorescence ratios of the different samples were plotted *versus* the respective pH values and results were fitted using Igor Pro 6.00 to obtain a calibration curve.

2.4.4 Effect of trapping laser and glucose exposure on internal pH. A 10 μL aliquot of cells loaded with SNARF-4F was injected in the microfluidic circuit and trapped in the cell channel containing McIllvaine buffer at pH 4. The array of trapped cells was moved to the reagent channel by translating the microfluidic chip using the scanning stage. To probe the effect of the trapping laser on the internal pH the cells were simply exposed to McIllvaine buffer at pH 4. To probe the effect of glucose on the internal pH the cells were exposed to a solution of 10 mM glucose in McIllvaine buffer at pH 4. Fluorescence images were taken every 30 s.

3 Results

3.1 Optical trapping and manipulation of yeast cells in microfluidics

In order to trap suspended yeast cells, the optical tweezer array was positioned in the cell channel (Fig. 1B) where the cells were passing at typical flowrates of 10–100 μm/s. The z-position (parallel to the optical axis) of the trap array was first roughly adjusted to ensure that most of the cells arrived below the focal plane of the optical traps. Then the z-position was fine-tuned until the trapping efficiency was optimal. Most of the traps in the array were usually filled in less than 1 min at appropriate particle densities (Movie1.mov†). Optical trapping of more than 200 yeast cells in parallel could be achieved (Fig. 2). The whole array of optically trapped cells could be moved within the microfluidic chip by translating the chip using the motorized scanning stage (Movie2.mov†).

Due to the Gaussian profile of the trapping laser impinging onto the microlens array, not all optical traps had the same power. Given a FWHM of 3 mm, an output power of 10 W of the trapping laser and the transmittance of 60% of the 40x microscope objective at the trapping laser wavelength of 1064 nm, the central tweezers disposed approximately 30 mW, while the peripheral ones only disposed 15 mW.

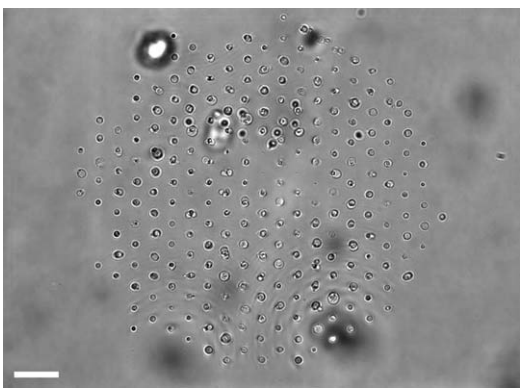

Fig. 2 Transmission micrograph of more than 200 optically trapped yeast cells; scale bar: 30 μm.

As the particles had to arrive in the focal plane to be trapped, only a subset of the particles traversing the optical tweezer array could usually be immobilized. To increase trapping efficiencies the height of the microfluidic channel was adjusted to 50 μm. Individual cells could be captured from the trap array and manipulated using the steerable optical trap. This opened the possibility to sort particles in the microfluidic chip for further analysis or incubation. A minimum fraction of 1% of the output power of the trapping laser was required for the steerable optical trap to capture cells from the trap array as, under this condition, the trapping force of the steerable trap substantially exceeded the trapping force of any of the optical traps in the array.

Cell sorting was accomplished through an interplay between the steerable trap and the syringe pump addressing the sorting channel. The pump was set in withdrawal mode and usually shut off when no cells were to be sorted. For sorting, the cell array was moved close to the sorting channel using the scanning stage. To avoid contamination of the sorting channel with cells that accidentally escaped their optical traps, the cell array was placed downstream to the sorting channel. Then a cell of interest was captured from the trap array, moved upstream the main channel to the entrance of the sorting channel, the steerable optical trap was switched off while the syringe pump was switched on to direct the particle into the channel (Fig. 3). The sorting procedure took typically 20–30 s, determined by the maximum rate at which the homebuilt galvanic mirror could be tilted, limiting the speed of the steerable optical trap to $\sim$ 10 μm/s.

3.2 Measurement of intracellular pH dynamics of optically trapped yeast cells following glucose exposure

The experimental platform was developed to provide a novel cytometric tool for parallelly screening the effects of chemical stimuli on single cells. To test and characterize the platform's applicability in single-cell studies the glucose-induced intracellular pH (pH_i) response of energy-starved yeast cells was chosen as a model system.

The intracellular pH is an important parameter of yeast physiology regulating various processes like cell metabolism and cell growth. Yeast pH_i is mainly controlled by the cell membrane H^+-ATPase, which during growth phase maintains the pH_i between 6 and 7.5 while the growth medium usually changes to lower extracellular pH (pH_e) values.[48–50] Yeast cells deprived of energy sources lack this ability to regulate their pH_i irrespective of the environment and therefore exhibit pH_i values in dependance of the external pH. Fig. 4 displays the relation between intracellular and extracellular pH of glucose-deprived cells. The intracellular pH can be measured using fluorescent probes such as SNARF-4F which can be calibrated *in situ* and offer ratiometric read-out of its fluorescence reducing artefacts. Two sets of experiments were performed: First, the pH_i of energy-starved yeast cells optically trapped over prolonged time periods was measured. These measurements serve as a blank for the glucose-sensing experiments and represent direct measurements of the effect of the trapping laser on yeast viability and vitality. The second set of experiments are the actual glucose-sensing experiments.

3.2.1 *In situ* calibration. In this study, the fluorescence ratio of SNARF-4F in Amphotericin-B treated yeast cells was measured

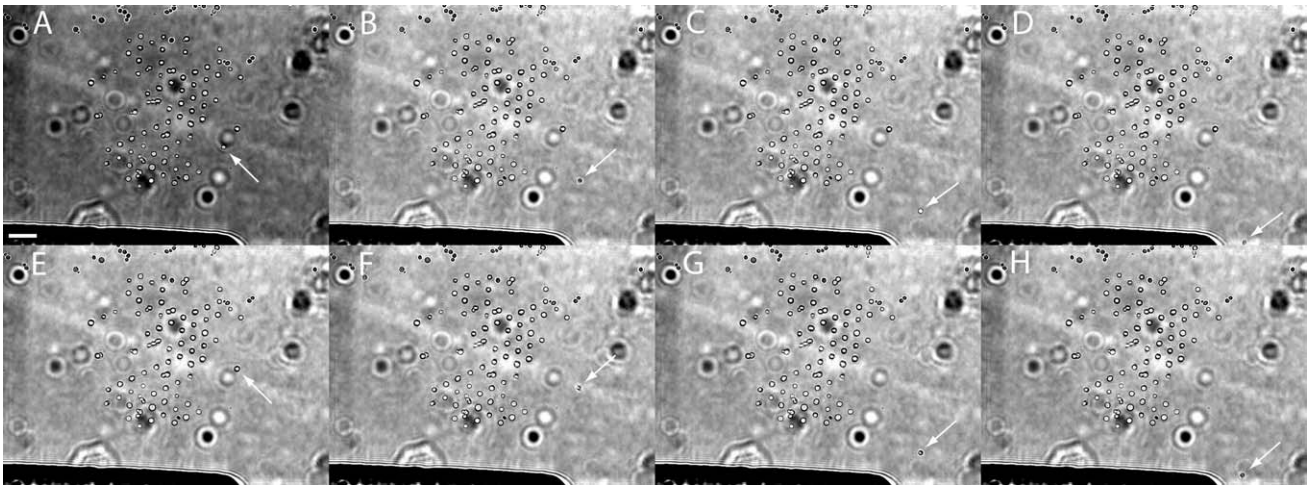

Fig. 3 (A-H) Sequence of transmission micrographs showing how two cells of interest (white arrows) are separated from an array of optically trapped yeast cells and isolated in the sorting channel; scale bar: 30 μm.

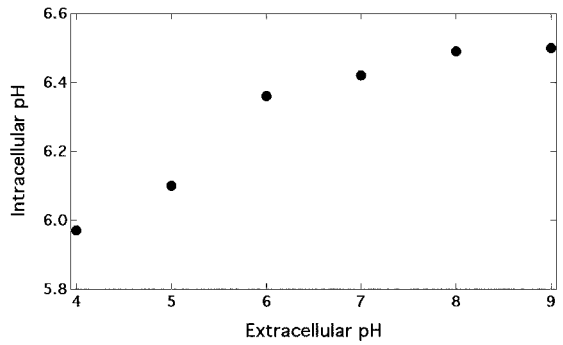

Fig. 4 Relation between intracellular and extracellular pH of energy-starved yeast cells.

versus known extracellular pH values. The antifungal drug Amphotericin B was used to permeabilise the yeast cell plasma membrane for protons.[48] After incubation of the yeast cells with Amphotericin B the intracellular pH adjusted to the extracellular pH. Fluorescence ratios (570 nm/670 nm) were plotted against extracellular pH values and the resulting calibration curve was fitted by a 2nd order polynomal function (Fig. 5).

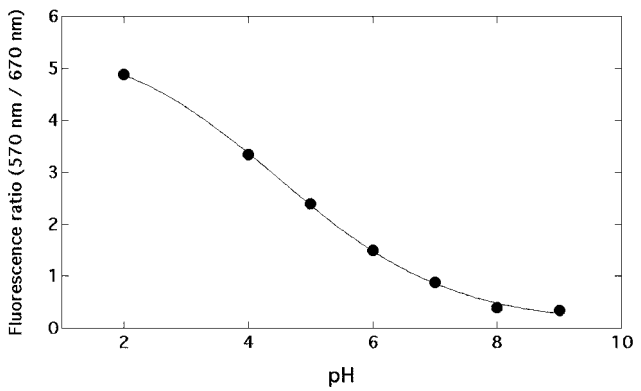

Fig. 5 Calibration curve plotting experimentally obtained SNARF-4F fluorescence ratios measured in Amphotericin B-treated yeast cells versus known extracellular pH values. The curve was fitted by a 2nd order polynomal function to experimental data.

3.2.2 Effect of optical trapping on intracellular pH. Measurement of the pH_i is considered to be a suitable method to assess yeast viability and vitality, *i.e.* to distinguish between dead and living cells, and between healthy and compromised cells, respectively.[51] Living cells are able to maintain a pH_i value close to pH 6, even in a low pH environment (Fig. 4). Dead cells, however, are unable to pump protons against a proton gradient and therefore will exhibit a pH_i equal to pH_e over the entire pH range.[52] The intracellular pH is also directly linked to a cell's vitality. A healthy cell will be able to maintain a high pH_i in a low pH environment, *e.g.* close to neutral pH, whereas a stressed cell will exhibit a smaller pH_i value.[51,53]

When yeast cells were not exposed to the trapping laser their pH_i remained stable over 15 min as monitored in cells that were sedimented in the reagent channel (data not shown).

The evolution of the pH_i in optically trapped cells is summarized in Fig. 6. About 50% of the cells in the trap array were sufficiently labeled with SNARF-4F to be distinguished from the background. Photobleaching of the dye could be minimized by proper adjustment of laser power and exposure time, artifacts based on remaining photobleaching could be eliminated by the ratiometric read-out. Initial pH values between 6 and 7 showed that all the cells under investigation were viable. Under trapping conditions the cells' vitality degraded through the influence of the trapping laser indicated by the continuous drop of pH_i seen in all the cells. However, it should be noted that even after 15 min of laser exposure the cells were still viable and capable of upholding a proton gradient. Due to the Gaussian beam profile of the trapping laser, cells in the center of the tweezer array were exposed to higher stress levels than cells in the periphery. Consequently, the intracellular pH of centrally trapped cells decreased to values between 5.0 and 5.5, whereas the intracellular pH of peripherally trapped cells only dropped to values between 5.5 and 6.0 (Fig. 6B).

3.2.3 Effect of glucose on intracellular pH. The dynamic response of pH_i of energy-starved yeast cells following glucose exposure is a phenomenon that has been already investigated elsewhere.[54–57] In these studies a shift towards higher pH_i values

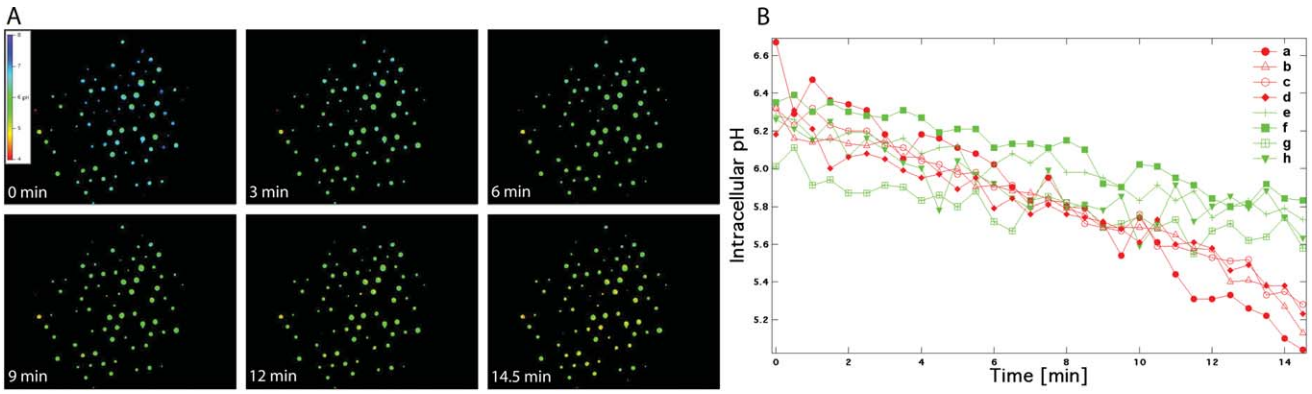

Fig. 6 (A) Sequence of fluorescence micrographs showing the temporal decrease of intracellular pH of optically trapped yeast cells induced by the trapping laser. Cells were glucose-deprived and trapped at pH 4. Intracellular pH was determined from the ratio of fluorescence intensities measured at 570 nm and 670 nm. (B) Temporal evolution of intracellular pH of 8 different cells from the array shown in A; (a–d) cells were trapped in the center of the optical tweezers array; (e–h) cells were trapped in the periphery of the optical tweezers array.

was observed when glucose at concentrations of 5–50 mM was delivered to the cells. The characteristics of this dynamic response depended on many factors like the type of yeast studied, its growth history and environmental conditions.

Here, we could reproduce the glucose-induced pH increase in optically trapped yeast cells (Fig. 7). Not all the cells reacted in the same way. Some cells responded within the first 2 min, others only after 3–4 min, some cells did not respond at all. Also did the pH_i response of individual cells differ in length and amplitude. Note that the pH_i of non-responding cells decreased according to the results shown in section 3.2.2. A decrease of SNARF-4F fluorescence was observed in one third of the labeled cells following glucose exposure. This is probably due to the yeast cells' efflux pumps activated by the availability of an external energy-source and actively expelling SNARF-4F molecules from the intracellular domain.[58] As a consequence of this effect, analysis of the results was restricted to the cells that retained the fluorophor. The dynamics of intracellular pH was also calculated as an average for the subset of 44 cells that were sufficiently labeled to be distinguished from the background (the total number of trapped cells was 98). This averaged response pattern outlines the results one would expect from ensemble measurements. It clearly shows that the transient rise of intracellular pH in individual cells is not recognized properly, on the one hand due to asynchronous behavior of responding cells, on the other hand due to the subset of cells that did not respond to glucose.

4 Discussion

We have developed a microfluidic array cytometer based on multiple optical traps generated by microlens arrays and demonstrated stable three-dimensional optical trapping of more than 200 living yeast cells in a microfluidic flow. Each of the trapped cells could be imaged simultaneously. To the best of our knowledge, this is the largest array of optically trapped yeast cells reported in literature. Refractive multiple optical tweezers have several advantages compared to diffractive methods like holographic tweezers and time-shared optical tweezers. First, microlens arrays have a higher optical throughput[46,59] and a high damage threshold offering the possibility to use high-power lasers for optical trapping. These are important requirements for creating large arrays of optical traps of sufficient stiffness for stable cell trapping and manipulation in microfluidics. Second,

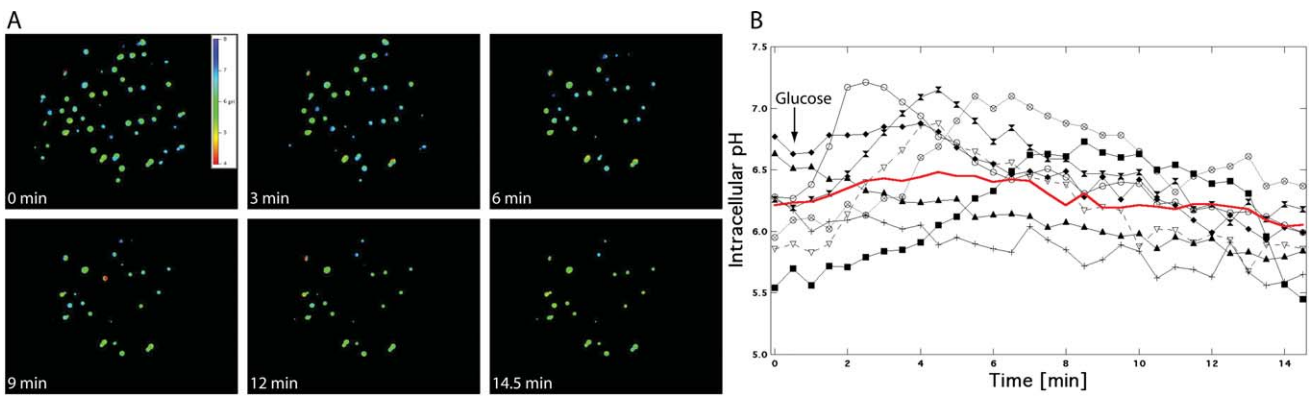

Fig. 7 (A) Sequence of fluorescence micrographs showing the temporal changes of intracellular pH of optically trapped yeast cells upon exposure of 10 mM glucose. Cells were glucose-deprived and trapped at pH 4. Intracellular pH was determined from the ratio of fluorescence intensities measured at 570 nm and 670 nm. (B) Temporal evolution of intracellular pH of 8 different cells from the array shown in A. The arrow indicates the timepoint of glucose exposure. The bold, red line represents the average response of 44 cells.

microlenses are low-cost and can be easily implemented into standard optical instruments. Individual particles in the fixed array can be manipulated by a steerable optical trap. The use of such a steerable optical trap allowed us to pick single cells out of their stable position in the trap array, to move them upstream and isolate them in a separate channel. An advantage of upstream sorting compared to usually employed downstream sorting consists in prevention of contaminating the sorting channel with untrapped particles. Following this procedure a throughput of 2–3 cells per minute could be achieved. Due to the low throughput, this sorting strategy will be hardly applicable when a large fraction of the cell population under investigation has to be sorted. Our sorting rate, however, is suited for applications where only a small subset of the cells are of interest. Note that our present sorting rate is determined by technical limitations of the employed galvanic mirror and is not an inherent limitation of the method. If fast sorting is a requirement, throughput might be increased using alternative approaches for generating steerable optical traps.[17,60]

The applicability of the array cytometer for studying dynamic responses in single cells was demonstrated in the present work by fluorescence ratio imaging of intracellular pH of each individual cell in the entire cell array. Monitoring the evolution of pH_i of optically trapped yeast cells in a low-pH environment was performed to measure the influences of the trapping laser on yeast viability. The results show that cells were stressed during 15 min exposure to the trapping laser, however, due to the unequal power distribution in the trap array, peripherally trapped cells were less stressed than centrally trapped cells. The observed relationship between applied laser power and accordingly induced cell stress is in agreement with similar studies on laser-trapped living cells.[61,62] These results indicated that, for the present experimental configuration, cell assays should not last longer than 15–20 min to avoid experimental artefacts caused by laser-induced cell stress and death. The fact that optically trapped cells are continuously exposed to stress imposes an upper limit for assay times defined by the applied laser power. Reducing the optical power per trap results in potentially longer assay times, but due to the then smaller trap stiffness greater care has to be taken for cell manipulation, and usually smaller flow rates have to be applied. Therefore, a tradeoff exists between assay time, applied laser power and liquid handling of the cell array, and these parameters have to be adjusted accordingly. Note that the use of laser sources emitting at wavelengths shorter than 1064 nm may reduce cell stress and in turn allow longer assay times.[63]

Exposure of starved yeast cells to glucose was followed by a transient rise of intracellular pH, which is in agreement with previous studies. However, a precedent acidification, reported by other groups,[54,55,64] could not be identified probably due to its fast kinetics. We have chosen this assay as it perfectly demonstrates the benefits of using high-density cell arrays combined with single cell analysis for the study of cellular dynamics. On the one hand, measurements were restricted to the small subset of cells that was sufficiently labeled and could retain the fluorophor over the whole measurement time (typically 10–20% of the cells). Since the cells were organized into a large and densely-packed array, this subset still contained at least 10–20 cells that could be sampled. Under these conditions, classical slide-based microscopy, where cells are randomely distributed in a loose manner and imaged through a high-resolution microscope objective of restricted field of view, often cannot sample enough cells to generate statistically significant results. On the other hand, the glucose-induced pH_i response pattern is highly dynamic and heterogeneous. Some cells responded almost immediately to the extracellular stimulus, while others responded only after 3–4 min or did not respond at all. Also did the response patterns differ in length and amplitude. While flow-cytometric methods would completely fail to resolve such differences of dynamics on a single-cell level due to the sub-second sampling time, our experimental platform allowed to sample the same cells over several minutes.

5 Conclusion

Our microfluidic array cytometer is of general interest to study variability of properties between individuals in an ensemble of live cells. It offers a number of features which could not be reached previously in functional studies of optically trapped living cells.[41,65,66] The multiple optical tweezers were capable to easily trap and monitor as individuals hundreds of cells simultaneously which yet was not achieved by alternative multiple optical trapping schemes. The implementation of an additional steerable trap allowed us to capture individual cells from the trapped array and to sort them within the microfluidic chip. Experimental platforms allowing to identify rare phenotypes with defined characteristics in a cell population and to subsequently isolate them for further analysis and/or cultivation are valuable tools for many areas of cell biological research.[3] Examples are clinical diagnostics, drug development or toxicity screening. We therefore plan to extend the presented array cytometer with additional on-chip functionalities allowing to further investigate sorted cells, *e.g.* using protein microarrays[67] or gene-expression analysis,[68] and multiplexing the investigation of single cells to the investigation of single vesicles derived from individual cells on our microfluidic chip.[69]

References

1 K. Cottingham, *Anal Chem*, 2004, **76**, 235A–238A.
2 C. E. Sims and N. L. Allbritton, *Lab Chip*, 2007, **7**, 423–40.
3 M. Leslie, *Science*, 2011, **331**, 24–6.
4 T. Y. Huang, T. F. Chu, H. I. Chen and C. J. Jen, *FASEB J*, 2000, **14**, 797–804.
5 W. J. Blake, M. Kaern, C. R. Cantor and J. J. Collins, *Nature*, 2003, **422**, 633–7.
6 L. Cai, N. Friedman and X. S. Xie, *Nature*, 2006, **440**, 358–62.
7 B. Huang, H. Wu, D. Bhaya, A. Grossman, S. Granier, B. K. Kobilka and R. N. Zare, *Science*, 2007, **315**, 81–4.
8 X. R. Bao, I. D. C. Fraser, E. A. Wall, S. R. Quake and M. I. Simon, *Biophys. J.*, 2010, **99**, 2414–22.
9 E. Kussell and S. Leibler, *Science*, 2005, **309**, 2075–8.
10 J. M. Raser and E. K. O'Shea, *Science*, 2005, **309**, 2010–3.
11 S. Tay, J. J. Hughey, T. K. Lee, T. Lipniacki, S. R. Quake and M. W. Covert, *Nature*, 2010, **466**, 267–71.
12 D. Wlodkowic and J. M. Cooper, *Anal. Bioanal. Chem.*, 2010, **398**, 193–209.
13 L. A. Herzenberg, D. Parks, B. Sahaf, O. Perez, M. Roederer and L. A. Herzenberg, *Clin Chem*, 2002, **48**, 1819–27.
14 L. A. Sklar, M. B. Carter and B. S. Edwards, *Curr. Opin. Pharmacol.*, 2007, **7**, 527–34.
15 A. Y. Fu, C. Spence, A. Scherer, F. H. Arnold and S. R. Quake, *Nat. Biotechnol.*, 1999, **17**, 1109–11.
16 S. C. Grover, A. G. Skirtach, R. C. Gauthier and C. P. Grover, *J. Biomed. Opt.*, 2001, **6**, 14–22.

17 M. M. Wang, E. Tu, D. E. Raymond, J. M. Yang, H. Zhang, N. Hagen, B. Dees, E. M. Mercer, A. H. Forster, I. Kariv, P. J. Marchand and W. F. Butler, *Nat. Biotechnol.*, 2005, **23**, 83–7.
18 J. Voldman, M. L. Gray, M. Toner and M. A. Schmidt, *Anal. Chem.*, 2002, **74**, 3984–90.
19 R. Pepperkok and J. Ellenberg, *Nat. Rev. Mol. Cell Biol.*, 2006, **7**, 690–6.
20 Y. Kuang, I. Biran and D. R. Walt, *Anal. Chem.*, 2004, **76**, 6282–6.
21 J. R. Rettig and A. Folch, *Anal. Chem.*, 2005, **77**, 5628–34.
22 S. Yamamura, H. Kishi, Y. Tokimitsu, S. Kondo, R. Honda, S. R. Rao, M. Omori, E. Tamiya and A. Muraguchi, *Anal. Chem.*, 2005, **77**, 8050–6.
23 K. Touhara, S. Sengoku, K. Inaki, A. Tsuboi, J. Hirono, T. Sato, H. Sakano and T. Haga, *Proc. Natl. Acad. Sci. U. S. A.*, 1999, **96**, 4040–5.
24 M. Hosokawa, A. Arakaki, M. Takahashi, T. Mori, H. Takeyama and T. Matsunaga, *Anal. Chem.*, 2009, **81**, 5308–13.
25 M. Emmert-Buck, R. Bonner, P. Smith, R. Chuaqui, Z. Zhuang, S. Goldstein, R. Weiss and L. Liotta, *Science*, 1996, **274**, 998–1001.
26 A. Revzin, K. Sekine, A. Sin, R. G. Tompkins and M. Toner, *Lab Chip*, 2005, **5**, 30–7.
27 R. M. Johann, *Anal. Bioanal. Chem.*, 2006, **385**, 408–412.
28 D. Wlodkowic, S. Faley, M. Zagnoni, J. P. Wikswo and J. M. Cooper, *Anal. Chem.*, 2009, **81**, 5517–23.
29 T. Kimura, Y. Sato, F. Kimura, M. Iwasaka and S. Ueno, *Langmuir*, 2005, **21**, 830–2.
30 J. Shi, D. Ahmed, X. Mao, S.-C. S. Lin, A. Lawit and T. J. Huang, *Lab Chip*, 2009, **9**, 2890–5.
31 P. Y. Chiou, A. T. Ohta and M. C. Wu, *Nature*, 2005, **436**, 370–2.
32 B. M. Taff and J. Voldman, *Anal. Chem.*, 2005, **77**, 7976–83.
33 M. Kirschbaum, M. S. Jaeger and C. Duschl, *Lab Chip*, 2009, **9**, 3517–25.
34 G. M. Akselrod, W. Timp, U. Mirsaidov, Q. Zhao, C. Li, R. Timp, K. Timp, P. Matsudaira and G. Timp, *Biophys. J.*, 2006, **91**, 3465–73.
35 C. Yi, C. Li, S. Ji and M. Yang, *Anal. Chim. Acta*, 2006, **560**, 1–23.
36 A. Ashkin, J. M. Dziedzic and T. Yamane, *Nature*, 1987, **330**, 769–71.
37 M. Ozkan, M. Wang, C. Ozkan, R. Flynn, A. Birkbeck and S. Esener, *Biomed. Microdevices*, 2003, **5**, 61–67.
38 P. Jordan, J. Leach, M. Padgett, P. Blackburn, N. Isaacs, M. Goksör, D. Hanstorp, A. Wright, J. Girkin and J. Cooper, *Lab Chip*, 2005, **5**, 1224–8.
39 A. Lafong, W. J. Hossack, J. Arlt, T. J. Nowakowski and N. D. Read, *Opt. Express*, 2006, **14**, 3065–72.
40 I. R. Perch-Nielsen, P. J. Rodrigo and J. Glückstad, *Proc. SPIE–Int. Soc. Opt. Eng.*, 2006, **6326**, 63261X–63261X-6.
41 E. Eriksson, D. Engström, J. Scrimgeour and M. Goksör, *Opt. Express*, 2009, **17**, 5585–94.
42 K. Visscher, G. J. Brakenhoff and J. J. Krol, *Cytometry*, 1993, **14**, 105–14.
43 K. Ramser and D. Hanstorp, *J. Biophotonics*, 2010, **3**, 187–206.
44 P. Rodrigo, R. Eriksen, V. Daria and J. Gluckstad, *Opt. Express*, 2003, **11**, 208–214.
45 C. Sow, A. Bettiol, Y. Lee, F. Cheong, C. Lim and F. Watt, *Appl. Phys. B: Lasers Opt.*, 2004, **78**, 705–709.
46 F. Merenda, J. Rohner, P. Pascoal, J.-M. Fournier, H. Vogel and R. P. Salathé, *Proc. SPIE–Int. Soc. Opt. Eng.*, 2007, **6483**, 64830A.
47 J. C. McDonald, D. C. Duffy, J. R. Anderson, D. T. Chiu, H. Wu, O. J. Schueller and G. M. Whitesides, *Electrophoresis*, 2000, **21**, 27–40.
48 M. Valli, M. Sauer, P. Branduardi, N. Borth, D. Porro and D. Mattanovich, *Appl. Environ. Microbiol.*, 2005, **71**, 1515–21.
49 K. Sigler, A. Knotková and A. Kotyk, *Biochim. Biophys. Acta, Biomembr.*, 1981, **643**, 572–82.
50 P. Eraso and C. Gancedo, *FEBS Lett.*, 1987, **224**, 187–92.
51 T. Imai and T. Ohno, *Appl Environ Microbiol*, 1995, **61**, 3604–8.
52 P. Breeuwer and T. Abee, *J. Microbiol. Methods*, 2000, **39**, 253–64.
53 C. Weigert, F. Steffler, T. Kurz, T. H. Shellhammer and F.-J. Methner, *Appl. Environ. Microbiol.*, 2009, **75**, 5615–20.
54 S. Ramos, M. Balbín, M. Raposo, E. Valle and L. A. Pardo, *J Gen Microbiol*, 1989, **135**, 2413–22.
55 M. T. A. P. Kresnowati, C. Suarez-Mendez, M. K. Groothuizen, W. A. van Winden and J. J. Heijnen, *Biotechnol. Bioeng.*, 2007, **97**, 86–98.
56 G. A. Martínez-Muñoz and P. Kane, *J. Biol. Chem.*, 2008, **283**, 20309–19.
57 R. Orij, J. Postmus, A. T. Beek, S. Brul and G. J. Smits, *Microbiology*, 2009, **155**, 268–78.
58 P. Breeuwer, J. L. Drocourt, F. M. Rombouts and T. Abee, *Appl Environ Microbiol*, 1994, **60**, 1467–72.
59 F. Merenda, J. Rohner, E. Lamothe, P. Pascoal, J.-M. Fournier and R.-P. Salathe, *Proc. SPIE–Int. Soc. Opt. Eng.*, 2007, **6644**, 66440P–66440P-10.
60 C. Mio, T. Gong, A. Terray and D. Marr, *Rev. Sci. Instrum.*, 2000, **71**, 2196–2200.
61 M. B. Rasmussen, L. B. Oddershede and H. Siegumfeldt, *Appl. Environ. Microbiol.*, 2008, **74**, 2441–6.
62 T. Aabo, I. R. Perch-Nielsen, J. S. Dam, D. Z. Palima, H. Siegumfeldt, J. Glückstad and N. Arneborg, *J. Biomed. Opt.*, 2010, **15**, 041505.
63 H. Liang, K. T. Vu, P. Krishnan, T. C. Trang, D. Shin, S. Kimel and M. W. Berns, *Biophys. J.*, 1996, **70**, 1529–33.
64 M. T. A. P. Kresnowati, C. M. Suarez-Mendez, W. A. van Winden, W. M. van Gulik and J. J. Heijnen, *Metab. Eng.*, 2008, **10**, 39–54.
65 E. Eriksson, J. Enger, B. Nordlander, N. Erjavec, K. Ramser, M. Goksör, S. Hohmann, T. Nyström and D. Hanstorp, *Lab Chip*, 2007, **7**, 71–6.
66 U. Mirsaidov, J. Scrimgeour, W. Timp, K. Beck, M. Mir, P. Matsudaira and G. Timp, *Lab Chip*, 2008, **8**, 2174–81.
67 S. Spisak, Z. Tulassay, B. Molnar and A. Guttman, *Electrophoresis*, 2007, **28**, 4261–73.
68 J. S. Marcus, W. F. Anderson and S. R. Quake, *Anal. Chem.*, 2006, **78**, 956–8.
69 P. Pascoal, D. Kosanic, M. Gjoni and H. Vogel, *Lab Chip*, 2010, **10**, 2235–2241.